

Ferromagnetic effects for peristaltic flow of Cu–water nanofluid for different shapes of nanosize particles

Noreen Sher Akbar¹ · Adil Wahid Butt¹

Received: 26 February 2015 / Accepted: 8 March 2015 / Published online: 28 March 2015
© The Author(s) 2015. This article is published with open access at Springerlink.com

Abstract In this study, tube flow of Cu–water nanofluid is considered with effect of different shaped nanoparticles. Hamilton–Crosser model is used for the effective thermal conductivity of the nanofluids. In addition, heat transfer through the tube is also studied for this problem. Exact solutions are obtained for governing modified equations with long wavelength and low Reynold number approximation case, and are discussed graphically.

Keywords Peristalsis · Heat transfer · Copper · Nanofluids · Shaped nanoparticles

Introduction

Peristalsis is a phenomenon in which a series of wave-like muscle contractions move the food to different stations in the digestive tract of a human body. The process of peristalsis begins when a bolus of food is swallowed and as a result, the strong wave-like motions of the smooth muscle in the esophagus carry the food to the stomach as the food then turns into chyme. This phenomenon is also involved in the intestines where the food is mixed and shifted back and forth. Latham (Latham 1966) was the first person to define the peristaltic pump. Soon after his significant work in 1966, many scientists and researchers turned their attention towards the experimental approach of peristaltic motion and peristaltic pumping. Barton and Raynor (1968) studied the peristaltic motion of a fluid in a tube and calculated the

time required for thyme to traverse unto the small intestines. Shapiro et al. (1969) studied peristaltic flow with long wavelength and low Reynolds number. Peristalsis attracted thousands of researchers around the globe due to its wide applications in the industry and in the field of medicine, i.e., the heart–lung machine. Interesting contribution towards peristalsis has been made since (Weinberg 1970; Sher Akbar 2015; Yin and Fung 1971; Sher Akbar and Butt 2015a; Vajravelu et al. 2007; Sher Akbar and Butt 2015b; Sher Akbar 2014).

The convective flow mechanisms of nanofluids are the subject of prominent work in this era. Current progress in nanotechnology introduced the use of fluids mixed with nanoparticles, called as nanofluids. The use of nanofluids in industries has become of great importance due to its applications, particularly the enhancement of thermal conductivity of a fluid (Rao 2010; Eastman et al. 2001; Choi et al. 2001; Xie et al. 2002; Xie et al. 2003; Sher Akbar et al. 2014; Sher Akbar and Butt 2014; Khan et al. 2014). Experimental study has shown that the effect that nanoparticles have on the enhancing the thermal conductivity depends on many circumstances including the shape and size of the nanoparticles. These nanofluids contain nanoparticles such as oxides, nitrides, metals or carbon nanotubes. The shapes of these nanoparticles may be different i.e., bricks, spheres, disks, or rods (Timofeeva et al. 2009). Based on the research of Maxwell (1873), Hamilton and Crosser (1962) found that the influence of particles shape can be accounted for using the sphericity of the particle. Further analysis could be seen through Refs. (Sher Akbar 2015a; Ellahi 2015; Sher Akbar 2014a; Mathur and He 2013; Sher Akbar 2015c; Gorji et al. 2014; Sher Akbar 2015d; Sher Akbar 2013; Sher Akbar 2014b).

In this article, we have studied the heat transfer characteristics of a nanofluid with different shaped

✉ Adil Wahid Butt
adil.maths86@gmail.com

¹ DBS&H, CEME, National University of Sciences and Technology, Islamabad, Pakistan

nanoparticles, using the Hamilton–Crosser model. The objective of this study is to analyze how the shapes of these nanoparticles effect towards the natural convection of the fluid under consideration. The problem is formulated using the Hamilton–Crosser model with heat transfer; the governing nonlinear differential equations are simplified using the low Reynolds number and long wavelength assumptions. Exact solutions are obtained for the velocity and temperature profile. Detailed discussion is presented over the subject with graphical description.

Formulation of the problem

Consider a non-Newtonian axisymmetric flow of copper nanofluids in a circular tube of finite length L . The inner surface of the circular tube is ciliated with metachronal waves and the flow occurs due to collective beating of the cilia. Heat transfer analysis with the nanofluid is also taken into account. A wave propagating wall of the tube has given a constant temperature T_0 (Fig. 1).

In the fixed coordinates (\bar{R}, \bar{Z}) , the flow between the two tubes is unsteady. It becomes steady in a wave frame (\bar{r}, \bar{z}) moving with the same speed as the wave moves in the \bar{Z} -direction. The transformations between the two frames are:

$$\begin{aligned}\bar{r} &= \bar{R}, \quad \bar{z} = \bar{Z} - c\bar{t}, \quad \bar{v} = \bar{V}, \quad \bar{w} = \bar{W} - c, \quad \bar{p}(\bar{z}, \bar{r}, \bar{t}) \\ &= \bar{p}(\bar{Z}, \bar{R}, \bar{t})\end{aligned}\quad (1)$$

The governing equations for an incompressible nanofluid can be written as:

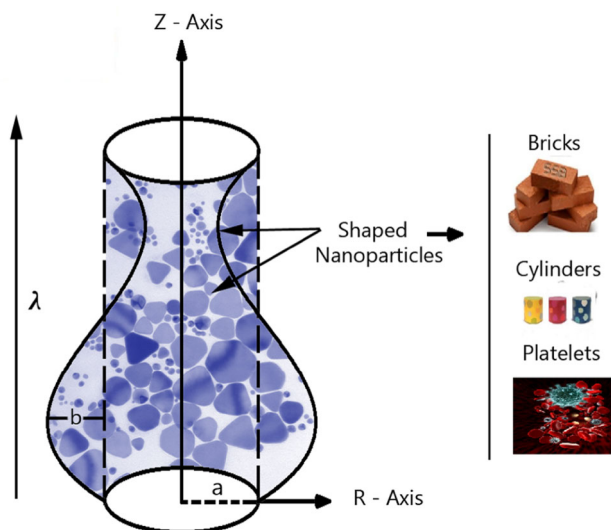


Fig. 1 Geometry of the Problem

$$\frac{1}{\bar{r}} \frac{\partial(\bar{r}\bar{u})}{\partial\bar{r}} + \frac{\partial\bar{w}}{\partial\bar{z}} = 0, \quad (2)$$

$$\begin{aligned}\rho_{nf} \left[\bar{u} \frac{\partial\bar{u}}{\partial\bar{r}} + \bar{w} \frac{\partial\bar{u}}{\partial\bar{z}} \right] &= -\frac{\partial\bar{P}}{\partial\bar{r}} + \mu_{nf} \frac{\partial}{\partial\bar{r}} \left[2 \frac{\partial\bar{u}}{\partial\bar{r}} \right] + \mu_{nf} \frac{2}{\bar{r}} \left(\frac{\partial\bar{u}}{\partial\bar{r}} - \frac{\bar{u}}{\bar{r}} \right) \\ &+ \mu_{nf} \frac{\partial}{\partial\bar{z}} \left[\left(\frac{\partial\bar{u}}{\partial\bar{r}} + \frac{\partial\bar{w}}{\partial\bar{z}} \right) \right],\end{aligned}\quad (3)$$

$$\begin{aligned}\rho_{nf} \left[\bar{u} \frac{\partial\bar{w}}{\partial\bar{r}} + \bar{w} \frac{\partial\bar{w}}{\partial\bar{z}} \right] &= -\frac{\partial\bar{P}}{\partial\bar{z}} + \frac{\mu_{nf}}{\rho_{nf}} \frac{\partial}{\partial\bar{z}} \left[2 \frac{\partial\bar{w}}{\partial\bar{z}} \right] + \mu_{nf} \frac{1}{\bar{r}} \frac{\partial}{\partial\bar{r}} \left[\bar{r} \left(\frac{\partial\bar{u}}{\partial\bar{z}} + \frac{\partial\bar{w}}{\partial\bar{r}} \right) \right] \\ &- \sigma B_o^2 (\bar{w} + c) + \rho_{nf} g \alpha (\bar{T} - T_0),\end{aligned}\quad (4)$$

$$(\rho_{cp})_{nf} \left(v \frac{\partial T}{\partial r} + w \frac{\partial T}{\partial z} \right) = k_{nf} \left[\frac{\partial^2 T}{\partial r^2} + \frac{1}{r} \frac{\partial T}{\partial r} + \frac{\partial^2 T}{\partial z^2} \right] + Q_0. \quad (5)$$

where r and z are the coordinates. z is taken as the center line of the tube and r transverse to it, u and v are the velocity components in the r and z directions, respectively, T is the local temperature of the fluid. Further, ρ_{nf} is the effective density, μ_{nf} is the effective dynamic viscosity, $(\rho_{cp})_{nf}$ is the heat capacitance, α_{nf} is the effective thermal diffusibility, and k_{nf} is the effective thermal conductivity of the nanofluid, which are defined as (see refs. Sher Akbar 2014; Sher Akbar and Butt 2014).



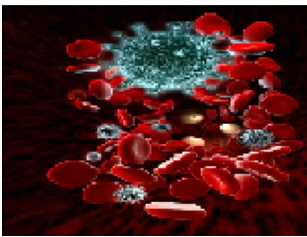
$$\begin{aligned}\rho_{nf} &= (1 - \phi) \rho_f + \phi \rho_p, \quad \mu_{nf} = \frac{\mu_f}{(1 - \phi)^{2.5}}, \\ \alpha_{nf} &= \frac{k_{nf}}{(\rho_{cp})_{nf}}, \quad (\rho_{cp})_{nf} = (1 - \phi) (\rho_{cp})_f + \phi (\rho_{cp})_p.\end{aligned}\quad (6a)$$

Here ϕ is the solid nanoparticle volume fraction. Maxwell (1873) and further developed Hamilton and Crosser model (1962) to take into account irregular particle geometries by introducing a shape factor. According to this model, when the thermal conductivity of the nanoparticles is 100 times larger than that of the base fluid, the thermal conductivity can be expressed as:

$$k_{nf} = k_f \left(\frac{k_s + (m + 1) k_f - (m + 1) (k_f - k_s) \phi}{k_s + (m + 1) k_f + \phi (k_f - k_s)} \right), \quad (6b)$$

where k_s and k_f are the conductivities of the particle material and the base fluid. In this Hamilton–Crosser model, m is the shape factor. The thermal conductivity and viscosity of various shapes of alumina nanoparticles in a fluid were investigated by Elena et al. (2009). They analyzed experimental data accompanied by theoretical modeling for different shapes of nanoparticles. According to them, the values of shape factor are given as in Table 1.

Table 1 Nanoparticle shape with their shape factor

Nanoparticles type	Shape	Shape factor
Bricks		3.7
Cylinders		4.9
Platelets		5.7

We introduce the following non-dimensional variables:

$$r = \frac{\bar{r}}{a}, \quad z = \frac{\bar{z}}{\lambda}, \quad w = \frac{\bar{w}}{c}, \quad u = \frac{\lambda \bar{u}}{ac}, \quad p = \frac{a^2 \bar{p}}{c \lambda \mu_f}, \quad \theta = \frac{(\bar{T} - \bar{T}_0)}{\bar{T}_0},$$

$$t = \frac{c \bar{t}}{\lambda}, \quad M^2 = \frac{\sigma B_0^2 a^2}{\mu_f}, \quad G_r = \frac{g \alpha a^2 T_0 \rho_{nf}}{c \mu_f}, \quad \xi = \frac{Q_0 a^2}{k_f T_0}. \quad (7)$$

Making use of these variables in Eqs. (2, 3, 4, 5), and using the assumptions of low Reynolds number and long wavelength, the non-dimensional governing equations after dropping the dashes can be written as:

$$\frac{\partial p}{\partial r} = 0, \quad (8)$$

$$\frac{dp}{dz} = \frac{1}{(1-\phi)^{2.5}} \frac{1}{r} \frac{\partial}{\partial r} \left(r \frac{\partial w}{\partial r} \right) - M^2(w+1) + G_r \theta, \quad (9)$$

$$0 = \frac{1}{r} \frac{\partial}{\partial r} \left(r \frac{\partial \theta}{\partial r} \right) + \xi \left(\frac{k_s + (m+1)k_f + \phi(k_f - k_s)}{k_s + (m+1)k_f - (m+1)(k_f - k_s)\phi} \right), \quad (10)$$

where M , ξ and G_r are the Hartmann number, heat absorption parameter and Grashof number respectively. The non-dimensional boundary conditions are given as:

$$\frac{\partial w}{\partial r} = 0, \quad \frac{\partial \theta}{\partial r} = 0 \quad \text{at } r = 0, \quad (11a)$$

$$w = -1, \quad \theta = 0, \quad \text{at } r = h(z) = 1 + \varepsilon \cos(2\pi z). \quad (11b)$$

Exact Solutions

Solving Eqs. (8, 9, 10) together with boundary conditions in Eq. (11a, 11b), we obtain:

$$w(r, z) = \frac{1}{4M^4 T} \left(\frac{4I_0 \left(rM \sqrt{(1-\phi)^{2.5}} \right) \left(G_r \xi + M^2 \frac{1}{(1-\phi)^{2.5}} \right)}{I_0 \left(hM \sqrt{T} \right)} - 4M^2(1-\phi)^{2.5} \left(M^2 + \frac{dp}{dz} \right) \right. \\ \left. + G_r \xi \frac{k_f}{k_{nf}} \left(M^2(h^2 - r^2)(1-\phi)^{2.5} - 4 \right) \right), \quad (12)$$

$$\theta(r, z) = \frac{1}{4} \left(\left(\frac{k_s + (m+1)k_f + \phi(k_f - k_s)}{k_s + (m+1)k_f - (m+1)(k_f - k_s)\phi} \right) \right) (h^2 - r^2) \xi. \quad (13)$$

The flow rate is given by:

$$F = 2 \int_0^{h(z)} r w dr, \quad (14)$$

this implies:

$$\frac{dp}{dz} = \frac{M \sqrt{(1-\phi)^{2.5}} I_0 \left(hM \sqrt{(1-\phi)^{2.5}} \right) \left(G_r h^2 \frac{k_f}{k_{nf}} \xi \left(h^2 M^2 (1-\phi)^{2.5} - 8 \right) - 8M^4 (F + h^2) (1-\phi)^{2.5} \right) + 16Gh \frac{k_f}{k_{nf}} \xi I_1 \left(hM \sqrt{(1-\phi)^{2.5}} \right)}{8h^2 M^3 \sqrt{(1-\phi)^{7.5}} I_2 \left(hM \sqrt{(1-\phi)^{2.5}} \right)}. \quad (15)$$

The pressure rise can be found by using the expression:

$$\Delta P = \int_0^1 \frac{dP}{dz} dz. \quad (16)$$

Results and discussions

The exact solutions obtained in the previous section have been discussed graphically for different physical parameters here. Figure 2 presents velocity profile for

different shapes of the nanoparticles i.e., Bricks, Cylinder and Platelets and also for different values of Hartmann number M . It is seen that when we increase Hartmann number M velocity field increases near the tube wall but decreases at the center of the tube. It is also seen that velocity when magnetic field is small for bricks particle is high and for cylinder particle is small, but as we increasing magnetic field then velocity for Platelets particle is high but for Bricks particle it is small. Figure 3 present pressure rise versus flow rate. It is observed that when we increase Hartmann number M pressure rise increases and pressure

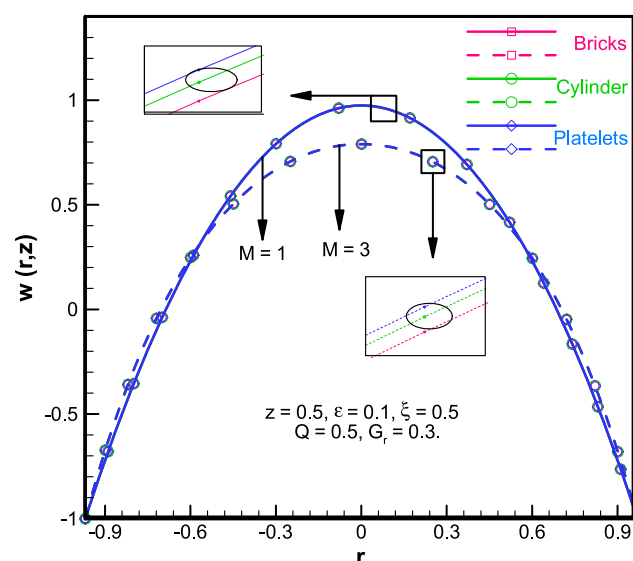


Fig. 2 Variation of velocity profile for different shape of the particle

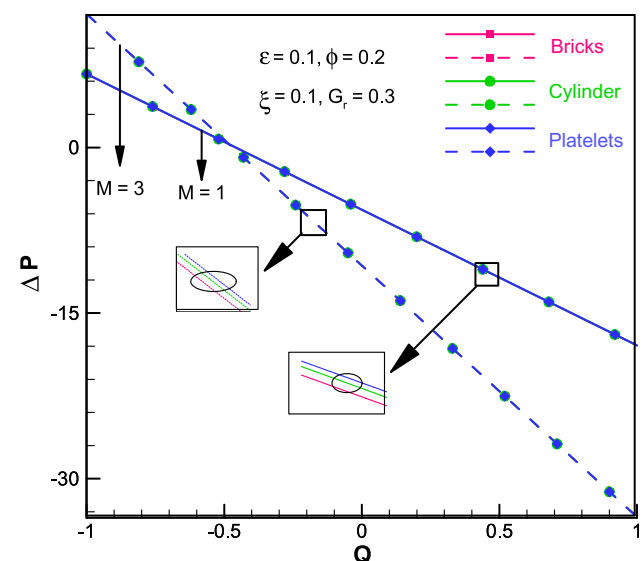


Fig. 3 Variation of pressure rise for different shape of the particle

to the thermal conductivity of the fluid. The higher the solid nanoparticle fraction the greater the thermal conductivity of the fluid.

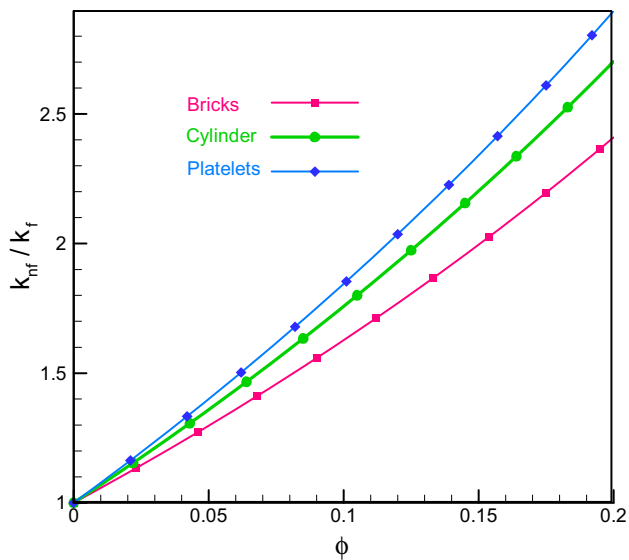


Fig. 4 Variation of effective thermal conductivity of the nanofluid for different shape of the particle

The effect of different shapes of nanoparticles on the temperature distribution is shown in Fig. 5a, b. The pictorial view indicates that temperature of the fluid inside the tube is greater at the center of the tube and significantly less at the walls of the tube. Temperature rises as we change the shape of nanoparticles from bricks to cylinders and platelets, respectively. Also we observe that temperature decrease with an increase in the heat absorption parameter ξ and it falls down when we increase ε . The thermal conductivity of the fluid improves if we use the particular brick shaped nanoparticles in the fluid.

Figure 6a, b are prepared to analyze the effect of different constraints on the pressure gradient. It is noticed that the pressure gradient has a sinusoidal behavior and it rises with a rise in the ratio of buoyancy forces to viscous forces i.e., Grashof number G_r , and its values drop significantly as the ratio of electromagnetic forces to viscous force increases i.e., Hartmann number M . Just like temperature rise, pressure gradient is also greater for platelets than that of cylinder and brick shaped nanoparticles.

Figure 7a, b, c are prepared to analyze the effect of cylinder and brick shaped nanoparticles on streamlines. It is observed that number of bolus for Bricks particles are

Fig. 5 Temperature profile $\theta(r, z)$ against the radial axis r for different values of ε and ξ

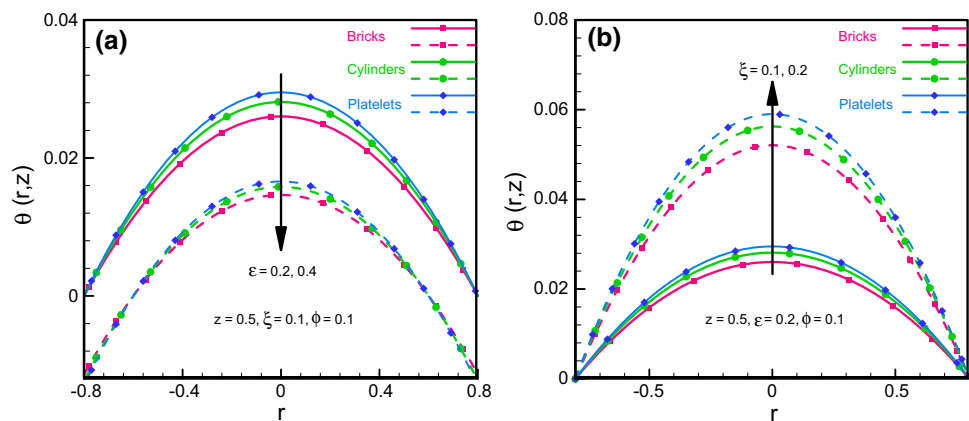
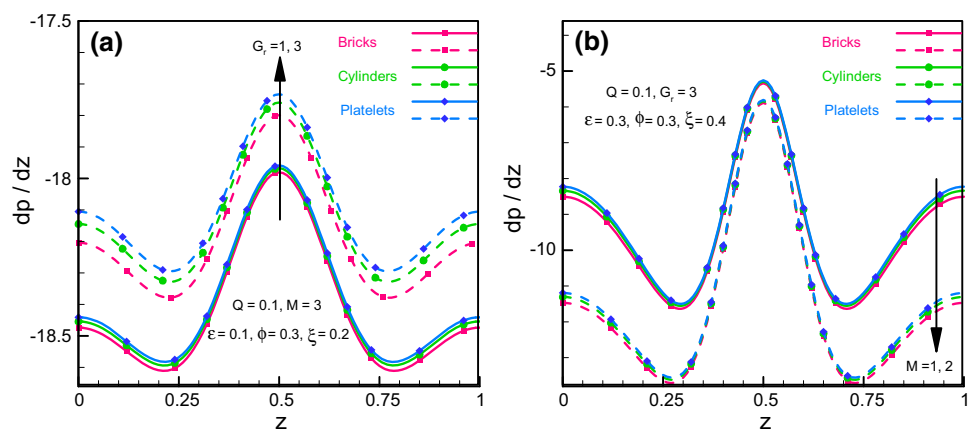


Fig. 6 Pressure gradient $\frac{dp}{dz}$ against the axial distance z for different values of G_r and M



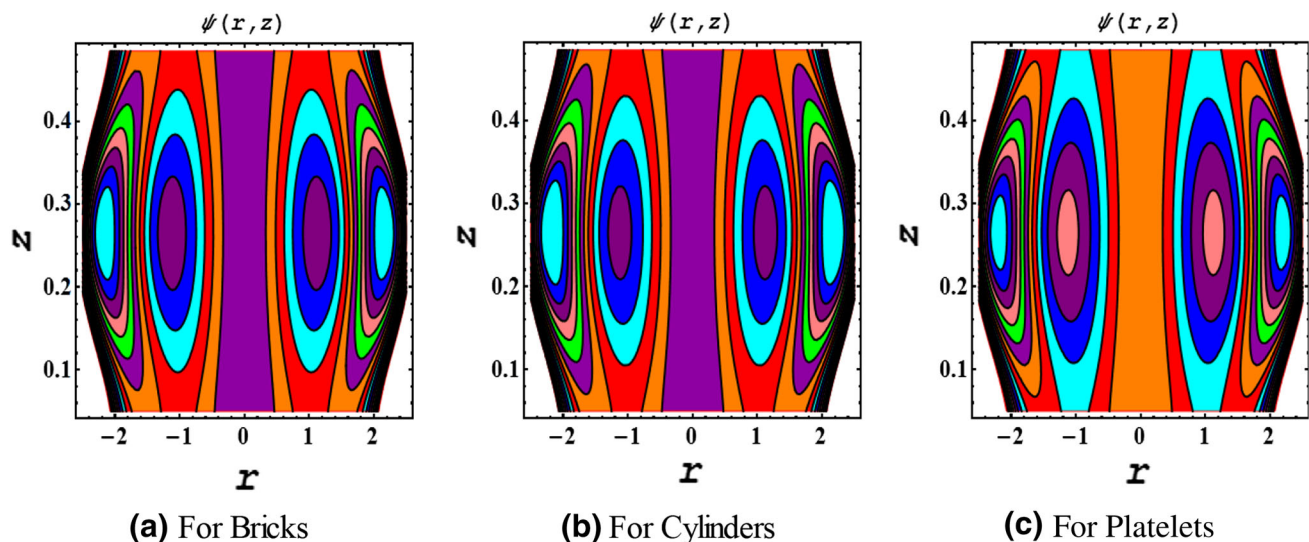


Fig. 7 Streamlines for different shape of the particle

high but size of the bolus for Bricks particle is small as compared to the Cylinder particles.

Conclusion

Tube flow of Cu–water nanofluid is considered with effect of different shaped nanoparticles. Hamilton–Crosser model is used for the effective thermal conductivity of the nanofluids.

1. It is seen that when we increase Hartmann number M velocity field increases near the tube wall but decreases at the center of the tube. It is also seen that velocity when magnetic field is small for Bricks particle is high and for cylinder particle is small.
2. It is observed that when we increase Hartmann number M pressure rise increases and pressure rise for Platelets case is high as compared to Bricks and Cylinder particles.
3. We can see a significant amount of difference in the thermal conductivities of different shape nanoparticles, with Platelets nanoparticles having the maximum thermal conductivity and Bricks nanoparticles having the least.
4. The solid nanoparticle volume fraction is directly proportional to the thermal conductivity of the fluid. The higher the solid nanoparticle fraction the greater the thermal conductivity of the fluid.
5. Temperature rises as we change the shape of nanoparticles from bricks to cylinders and platelets respectively.
6. It is noticed that the pressure gradient is also greater for platelets than that of cylinder and brick-shaped nanoparticles.

7. It is observed that number of bolus for Bricks particles are high but size of the bolus for Bricks particle is small as compared to the Cylinder particles.

Open Access This article is distributed under the terms of the Creative Commons Attribution License which permits any use, distribution, and reproduction in any medium, provided the original author(s) and the source are credited.

References

- Barton C, Raynor S (1968) Peristaltic flow in tubes. *Boll Math Biophys* 30:663–680
- Choi SUS, Zhang ZG, Yu W, Lockwood FE, Grulke EA (2001) Anomalous thermal conductivity enhancement in nanotube suspensions. *Appl Phys Lett* 79(14):2252–2254
- Eastman JA, Choi SUS, Yu W, Thompson LJ (2001) Anomalous increased effective thermal conductivity of ethylene glycol-based nanofluids containing copper nanoparticles. *Appl Phys Lett* 78(6):718–720
- Ellahi R (2015) Shape effects of nanosize particles in Cu-H₂O nanofluid on entropy generation. *Int J Heat Mass Transf* 81:449–456
- Gorji S, Seddighi M, Ariyaratne C, Vardy AE, O'Donoghue T, Pokrajac D, He S (2014) A comparative study of turbulence models in a transient channel flow. *Comput Fluids* 89:111–123
- Hamilton RL, Crosser OK (1962) Thermal conductivity of heterogeneous two-component system. *Ind Eng Chem Fundam* 1(1):187–191
- Khan U, Ahmed N, Khan SIU, Mohyud-din ST (2014) Thermo-diffusion effects on MHD stagnation point flow towards a stretching sheet in a nanofluid. *J Propul Power* 3(3):151–158
- Latham TW (1966) Fluid motion in a peristaltic pump. MS. Thesis, Massachusetts Institute of Technology, Cambridge
- Mathur A, He S (2013) Performance and implementation of the Launder-Sharma low-Reynolds number turbulence model. *Comput Fluids* 79:134–139
- Maxwell JC (1873) *A Treatise on Electricity and Magnetism*. Clarendon Press, Oxford

- Rao Y (2010) Nanofluids: stability, phase diagram, rheology and applications. *Particuology* 8(6):549–555
- Sher Akbar N (2014a) Nanofluid analysis for the intestinal flow in a symmetric channel. *IEEE Trans Nanobiosci* 13(4):1–5
- Sher Akbar N (2014b) Peristaltic Sisko Nano fluid in an asymmetric channel. *Appl Nanosci* 4:663–673
- Sher Akbar N (2015a) Influence of magnetic field on peristaltic flow of a Casson fluid in an asymmetric channel: Application in crude oil refinement. *J Magn Magn Mater* 378:320–332
- Sher Akbar N (2015b) Heat transfer and carbon nano tubes analysis for the peristaltic flow in a diverging tube. *Meccanica* 50:39–47
- Sher Akbar N (2015c) Application of Eyring-Powell fluid model in peristalsis with nano particles. *J Comput Theor Nanosci* 12:94–100
- Sher Akbar N (2015d) Biological analysis of nano Prandtl fluid model in a diverging tube. *J Comput theor Nanosci* 12:105–112
- Shapiro AH, Jaffrin MY, Weinberg SL (1969) Peristaltic pumping with long wavelengths at low Reynolds number. *J Fluid Mech* 37:799–825
- Sher Akbar N (2013) MHD peristaltic flow of a nanofluid with Newtonian heating. *Curr Nanosci* 10:863–868
- Sher Akbar N (2014c) Peristaltic flow of tangent hyperbolic fluid with convective boundary condition. *Eur Phys J Plus* 129:214
- Sher Akbar N, Butt AW (2014) CNT suspended nanofluid analysis in a flexible tube with ciliated walls. *Eur Phys J Ap* 129:174
- Sher Akbar N, Butt AW (2015a) Heat transfer analysis for the peristaltic flow of Herschel–Bulkley fluid in a nonuniform inclined channel. *Zeitschrift für Naturforschung A*. 70:23–32
- Sher Akbar N, Butt AW (2015b) Physiological transportation of casson fluid in a plumb duct. *Commun Theor Phys* 63:347–352
- Sher Akbar N, Butt AW, Noor NFM (2014) Heat transfer analysis on transport of copper nanofluids due to metachronal waves of cilia. *Curr Nanosci* 10(6):807–815
- Timofeeva EV, Roubort JL, Singh D (2009) Particle shape effects on thermophysical properties of alumina nanofluids. *J Appl Phys* 106:014304
- Vajravelu K, Radhakrishnamacharya G, Radhakrishnamurthy V (2007) Peristaltic flow and heat transfer in a vertical porous annulus with long wave approximation. *Int J Nonlinear Mech* 42:754–759
- Weinberg SL (1970) Theoretical and experimental treatment of peristaltic pumping and its relation to ureteral function, Ph.D. Thesis, Massachusetts Institute of Technology, Cambridge
- Xie H, Wang J, Xi T, Liu Y (2002) Thermal Conductivity of Suspensions Containing Nanosized SiC Particles. *Int J Thermo-phys* 23(2):571–580
- Xie H, Lee H, Youn W, Choi M (2003) Nanofluids containing multiwalled carbon nanotubes and their enhanced thermal conductivities. *J Appl Phys* 94(8):4967–4971
- Yin FCP, Fung YC (1971) Comparison of theory and experiment in peristaltic transport. *J Fluid Mech* 47(1):93–112